

CatchBackdoor: Backdoor Testing by Critical Trojan Neural Path Identification via Differential Fuzzing

Haibo Jin, Ruoxi Chen, Jinyin Chen, Yao Cheng, Chong Fu, Ting Wang, Yue Yu, and Zhaoyan Ming

Abstract—The success of deep neural networks (DNNs) in real-world applications has benefited from abundant pre-trained models. However, the backdoored pre-trained models can pose a significant trojan threat to the deployment of downstream DNNs. Existing DNN testing methods are mainly designed to find incorrect corner case behaviors in adversarial settings but fail to discover the backdoors crafted by strong trojan attacks. Observing the trojan network behaviors shows that they are not just reflected by a single compromised neuron as proposed by previous work but attributed to the critical neural paths in the activation intensity and frequency of multiple neurons. This work formulates the DNN backdoor testing and proposes the CatchBackdoor framework. Via differential fuzzing of critical neurons from a small number of benign examples, we identify the trojan paths and particularly the critical ones, and generate backdoor testing examples by simulating the critical neurons in the identified paths. Extensive experiments demonstrate the superiority of CatchBackdoor, with higher detection performance than existing methods. CatchBackdoor works better on detecting backdoors ($\sim \times 1.5$) by stealthy blending and adaptive attacks, which existing methods fail to detect. Moreover, our experiments show that CatchBackdoor may reveal the potential backdoors of models in Model Zoo. Besides, by retraining models with the testing examples generated by CatchBackdoor, the models' robustness against trojan attacks is improved by up to 60%.

Index Terms—Deep neural network, trojan attacks, backdoor testing, neural path.



1 INTRODUCTION

Over the past few years, deep neural networks (DNNs) have made significant progress in solving complex learning tasks [1], [2], [3] with outstanding accuracy. Training a powerful DNN is usually extremely time-consuming, so adopting a pre-trained model has become the mainstream to improve efficiency. Suppliers and developers distribute, share, reuse, and even sell pre-trained models for profit, e.g., Model Zoo [4] with thousands of pre-trained models for free download. We benefit from these convenient pre-trained models, but are also threatened by serious security problems, i.e., unknowingly downloading a trojaned model. It has been revealed that deep models, es-

pecially the pre-trained models, are susceptible to trojan manipulations, such as their training set [5], [6], [7] and model parameters [8]. Specifically, such models will expose wrong/targeted prediction when the backdoor is triggered in the inference stage, namely trojan attack on DNNs. It is of great importance to conduct backdoor testing to responsibly rely critical tasks on DNNs [9].

According to the definition of trojan attacks [10], the model with backdoors exposes trojaned behaviors only when the input contains the trigger. Therefore, the key to determining whether the model is trojaned lies in whether testing methods can effectively find the triggers and lead to trojan behaviors of models during the testing stage. However, existing DNN testing methods, are mainly designed for evaluating DNN models against adversarial examples. Some borrow the idea of code coverage [11], [12] in software testing [13], [14], [15], and use neurons' activation status to gauge the exploration of the input. Based on the observation that neurons' activation on adversarial examples is higher than that of the benign ones, Ma et al. [16] proposed six coverage-based metrics for generating testing examples to hunt adversarial attacks. Along the line, we applied it to trojan testing of DNN and found that neuron activation behaviors for trojaned and benign examples are almost the same during the testing phase; consequently, none of the neuron coverage-based metrics succeeds for backdoor testing (more in Fig. 5).

Like and yet distinct from trojan testing, backdoor detection is designed to detect the potential backdoor inside the model without considering example generation diversity. Numerous backdoor detection techniques have been proposed [17], [18], [19], [20], [21], [22]. However, they

- This research was supported by the National Natural Science Foundation of China under Grant No. 62072406, the Natural Science Foundation of Zhejiang Provincial under Grant No. LY19F020025.
- H. Jin and R. Chen are with the College of Information Engineering at Zhejiang University of Technology, Hangzhou 310007, China. (e-mail: 2112003149@zjut.edu.cn, 2112003035@zjut.edu.cn).
- J. Chen is with the Institute of Cyberspace Security, College of Information Engineering, Zhejiang University of Technology, Hangzhou, 310023, China. (e-mail: chenjinyin@zjut.edu.cn)
- Y. Cheng is with the Huawei International, Singapore (email: chengyao101@huawei.com)
- C. Fu is with the College of Computer Science and Technology at Zhejiang University, Hangzhou 310007, China. (email: fuchong@zju.edu.cn)
- T. Wang is with Pennsylvania State University, USA (email: inbox.ting@gmail.com)
- Y. Yue is with the Key Laboratory of Parallel and Distributed Computing, College of Computer, National University of Defense Technology, Changsha, 410000, China. (email: yuyue@nudt.edu.cn)
- Z. Ming is with Zhejiang University City College, Hangzhou, China. (email: mingzhaoyan@gmail.com)

Manuscript received xx xx, 2021; revised xx xx, xxxx.

have shown limitations in detecting advanced trojan attacks, especially blending attacks [6], [7] and defense adaptive attacks [10], [23]. For instance, artificial brain stimulation (ABS) [17], the state-of-the-art (SOTA) backdoor detection method, achieves satisfying performance, assuming that a single compromised neuron is responsible for the trojaned behavior. Usually, activation values of the neuron will increase dramatically when triggered by modification attacks [5], [24], [25]. However, in strong attacks such as blending attacks [7], [26], [27], where neuron activation value remains relatively constant, ABS fails to find compromised neurons. (refer to the experiment result in Fig. 1).

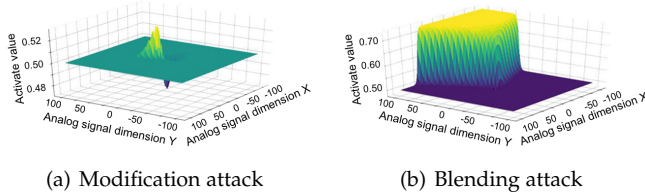


Fig. 1. The change of neuron activation value with analog signal input after certain stimulation of the MNIST [28] on LeNet-5 [29] model. Modification attack [5] based on 3×3 fixed-position patches and blending attack are implemented for comparison.

Since one single neuron’s activation value cannot well reflect trojan attack’s behaviors, there is still a gap between trojan attacks and neuron behaviors. To bridge the gap, we introduce the concept of *neural path* for the first time, by linking the critical neurons, i.e., neurons of the larger activation values and higher frequency. Neural path represents the data flow along the path, and the neuron behaviors within the model that are most relevant to the decision.

We conduct a study on how neuron paths are different for benign and trojan examples. We found that benign examples with different labels stimulate different benign neural paths, i.e., benign neural paths, benign path for short. However, when trojan examples crafted based on these benign examples, they all activate a similar neural path different from the benign neural paths.

An example of a 4-layer trojaned model trained on ImageNet [30] is shown in Figure 2. The trigger is a reversed λ and any input with this trigger can be highly predicted to the target label, i.e., Tabby cat. We visualize the neural path using a class of images, i.e., Siberian husky. The green, blue and orange colors are for benign examples, transition examples (the example with part of trigger, but cannot trigger the target prediction) and trojaned examples, respectively. We notice that the transition neural path approaches the trojan neural path, in terms of activation values and activation frequency. With more and more parts of trigger on the examples, their transition path gradually approaching the trojan path. Once they are close enough, the backdoor behavior will be triggered.

We can understand this observation in that the trojan trigger leads to a type of trojan behavior by stimulating the trojan path. Consequently, by modifying the input, the path can be forced to approach the trojan path, thereby effectively generating reverse triggers. Motivated by this insight, we design a backdoor testing method. We fuzz the benign neural path to approximate a potential trojan path. Then, potential trojan triggers that can trigger the trojan behaviors

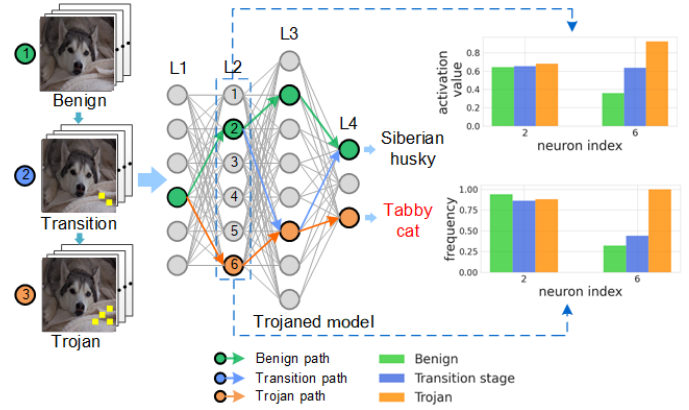


Fig. 2. Neural paths simulated by benign and trojan examples. Bars with green, blue and orange denote neuron activation value and the activated frequency of neurons in layer 2 from benign to trojan.

can be generated by reversing the trojan path from given input examples.

We count the number of examples containing the triggers reversed by our method leading to a different prediction label from the original prediction label. If the number exceeds a certain threshold, there is a high probability that the model has a backdoor (can be implanted or nature) that can be triggered by a certain trigger (can be in input space or representation space).

Our main contributions are summarized as follows.

- We find the intrinsic trojaned DNN behaviors manifested by a path of highly and frequently activated neurons via differential fuzzing. For the first time, we define and formalize it as the Critical Trojan Neural Path.
- We propose **CatchBackdoor**, a novel trojan testing framework based on testing examples generated by the Critical Trojan Neural Paths. It hunts trojans in DNN models 2.3 times better than existing methods.
- Re-training the model using the generated backdoor testing examples can effectively repair the backdoor model. The model’s robustness against trojan attacks improves by up to 60%, better than the SOTA methods.

2 CATCHBACKDOOR

2.1 Preliminaries

This subsection presents basic notations and definitions for better understanding of CatchBackdoor.

Notations. Trojan trigger is a specific pattern generated by attackers to trigger trojaned behaviors. An example containing a trojan trigger is defined as a trojan example. There are many approaches to implant a trojan trigger to a model [5], [23], [31]. Trojaned behaviors, i.e., misclassifications, will be triggered when a trojaned model is fed with trojan examples.

Backdoor detection is an approach designed to detect the potential backdoor in the model without considering example generation efficiency. Backdoor testing triggers corner-case behaviors by generating diverse testing examples with

efficiency and high coverage. Neural paths stimulated by benign examples are called benign paths, while those stimulated by trojan examples are named trojan paths.

Definition 1 (Neuron Contribution). Given a DNN with its input example $x \in X$, where $X = \{x_1, x_2, \dots\}$ and loss function $\mathcal{L}(\cdot)$. We introduce a function $\varphi(n_{i,j}, x)$ that measures the output of j -th neuron $n_{i,j}$ in i -th layer. The neuron contribution of $n_{i,j}$ is calculated as:

$$\xi(n_{i,j}, x) = \frac{\partial \mathcal{L}(x)}{\partial \varphi(n_{i,j}, x)} \quad (1)$$

where $\xi(n_{i,j})$ denotes the neuron contribution. It reflects the influence of neuron activation value to model decision. ∂ denotes the partial derivative function.

Definition 2 (Critical Neurons). Given a l -layer DNN, we take neurons from the input layer as the start and those from the output layer as the end. Critical Neurons are a set of neurons in the hidden layers, defined as follows:

$$\text{Critical Neurons}(x) = \bigcup_{i=1}^{l-1} \bigcup_{j=1}^k n_{i,j} \quad (2)$$

where $n_{i,j}$ denotes the j -th neuron in i -th layer of the DNN and k denote the number of chosen neurons. Neurons with larger activation values and higher frequency will be selected and included in this aggregation, i.e., usually top- k neurons in each layer are chosen.

Definition 3 (Data Flow). We define the direction of data flow from neuron $n_{i,j}$ to $n_{i+1,j}$ in a given DNN as:

$$\text{Data Flow}(n_{i,j}, n_{i+1,j}) : w^{(i,j)} \rightarrow w^{(i+1,j)} \quad (3)$$

Data flow reflects the direction of weight in the forward propagation and represents the connection relationship between neurons.

Definition 4 (Neural Path). Given critical neurons and data flow, for input $x \in X$, the neural path can be defined as:

$$\text{Neural Path}(x) = \bigcup_{i=1}^{l-1} \bigcup_{j=1}^k \{n_{i,j}, \text{Data Flow}(\cdot)\} \quad (4)$$

where $n_{i,j} \in \text{Critical Neurons}$ and $i < l$ denotes i -th layer of the DNN. The neural path links neurons along with the data flow between them.

2.2 Proposed CatchBackdoor Framework

The framework of CatchBackdoor is shown in Figure 3, including five main steps: ①the benign path construction, ②critical trojan neural path identification, ③reversed trigger generation and ④testing example generation, and ⑤DNN trojan detection. More specifically, a benign seed is an input example (e.g., a benign input or a noise input) that can be used to construct the benign neural path. By fuzzing the benign neural paths, CatchBackdoor obtains trojan neural paths and then reverses the trojan paths to construct triggers. Testing examples are generated by adding reversed triggers to the benign seeds. These testing examples along with the benign seeds are fed into the model to be tested and CatchBackdoor monitors whether there is a change in the model prediction. CatchBackdoor determines

whether a model is trojaned by calculating the label change rate (LCR), i.e., a larger LCR indicates a higher probability that the model is trojaned. The pseudo-code of generating testing examples is presented in **Algorithm 1**. The following subsections explain details of each step.

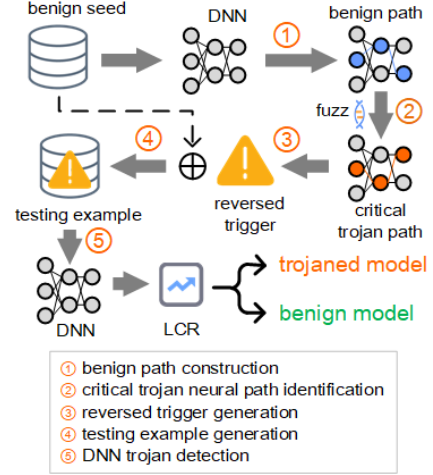


Fig. 3. CatchBackdoor Framework for DNN testing of trojaned models.

2.3 Benign Path Construction

We use benign seeds to search critical neurons with large activation values and high frequency. By linking these neurons, benign path can be constructed according to the neuron contribution. The workflow is shown in Figure 4, where top- k neurons in each layer are linked to form the benign path. As the color goes deeper, the activation values of neurons increase. "FC" denotes the fully connected layer.

Given a benign example $x \in X$, where $X = \{x_1, x_2, \dots\}$ denotes a set of benign examples, we select neurons based on their activation status from x .

We denote $A_{i,j} \in \mathbb{R}^{H \times W \times C}$ as the *feature map* activation of j -th feature map in the i -th convolutional layer, where H, W, C represent the height, width and channel. Global average pooling (GAP) is adopted on the raw feature map $A_{i,j}$ to obtain the channel-wise activation $\phi'(x)$, calculated as follows:

$$\phi'(x) = \frac{1}{H \times W} \sum_W \sum_H A_{i,j} \quad (5)$$

GAP is used on each convolutional layer and pooling layer while the output of fully connected layers is left undone.

Then we calculate the neuron contribution of each neuron in the model according to Equation 1 and arrange them in descending order. k neurons frequently ranked top are selected as critical neurons. They have larger activation values, and hence are considered to have higher contribution to model's decision. Specifically, k_1 are used for convolutional layers and k_2 for fully connected layers to achieve a balance between high-level semantics and detailed spatial information. By linking neurons and the data flow among them, the benign path is constructed, denoted as *Benign Path_x*.

2.4 Critical Trojan Neural Path Identification

According to our observation, trojan behaviors are highly related to the activation of trojan paths which are stimulated

Algorithm 1 Generation of testing examples

Input: Benign seeds $X = \{x_1, x_2, \dots\}$. Trigger size μ . LCR threshold $\lambda=0.5$. Top- k selection coefficient. Iteration step s . And maximum number of iterations S . The set of neural path H during iterations.

Output: Generated testing examples $T = \{x_{t1}, x_{t2}, \dots\}$

```

1:  $T = \{\emptyset\}, H = \{\emptyset\}$ 
2: for  $x$  in  $X$  do
3:    $Critical\ Neurons \leftarrow$  Select Top- $k$  Neurons in each
     layers according to Equation 1
4:   Construct  $Benign\ Path(x)$  according to Equation 4
5:   for  $s$  in  $S$  do
6:     Update  $Trojan\ Path(x)$  according to Equation 6
7:     if Stable Condition according to Equation 7 then
8:       Break
9:     else
10:       $H \leftarrow H \cup Trojan\ Path(x)$ 
11:    end if
12:  end for
13:   $Critical\ Trojan\ Neurons(x) \leftarrow$  Select top- $k$  neurons
     in each layer according to Equation 8
14:  Construct  $Critical\ Trojan\ Path(x)$  according to
     Equation 4
15:  Generate  $x_t$  according to Equation 9 and 10
16:   $T \leftarrow T \cup x_t$ 
17: end for
  
```

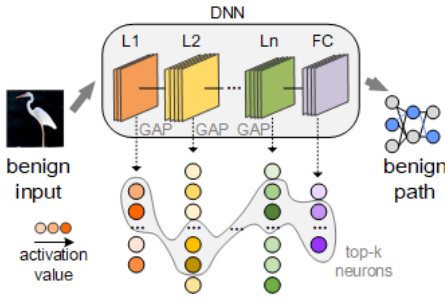


Fig. 4. Benign path construction.

by trojan triggers. By fuzzing the benign path stimulated by benign examples, it will gradually approach the trojan paths and finally become the cortical trojan neural path. Specifically, we maximize the activation of each neuron on the benign path to enlarge their contributions. The fitness function of this process can be formalized as,

$$Fitness = \max(\xi(n_{i,j})), \forall n_{i,j} \in Trojan\ Path(x) \quad (6)$$

where $Trojan\ Path(x)$ denotes the trojan path with the input x .

After S rounds of iteration, we can get S trojan paths, the aggregation of which can be denoted as $H = \{Trojan\ Path(x)_1, Trojan\ Path(x)_2, \dots, Trojan\ Path(x)_S\}$. When the neurons on the $Trojan\ Path(x)$ no longer change, we consider the process is converged, i.e., a potential trojan path is found. Hence, we early stop any unnecessary further

iteration once the below condition is met.

$$Trojan\ Path(x)_s = Trojan\ Path(x)_{s-1}, \quad (7)$$

$$\forall n_{i,j} \in Trojan\ Path(x)_s, Trojan\ Path(x)_{s-1}$$

where $s, s-1 < S$, is the intermediate process of iteration.

Then, we calculate the frequency of each neuron in each neural path from set H . Intuitively, neurons with higher frequency in multiple paths make the most significant contributions. We select the top- k neurons, namely critical trojan neurons, to compose critical trojan path, defined as follows.

$$Critical\ Trojan\ Neurons(x) = \bigcup_{i=1}^{l-1} \bigcup_{j=1}^k \arg \max_{n_{i,j} \in H} f(n_{i,j}, x) \quad (8)$$

where $f(\cdot)$ is the frequency of neurons. \bigcup represents the aggregation of chosen neurons in multiple $Trojan\ Path$ after the S -round iteration process.

We link critical trojan neurons with data flow to become a critical trojan path, denoted as $Critical\ Trojan\ Path(x)$.

2.5 Testing Example Generation

In order to generate testing examples, we need to reverse the triggers first. For an input benign seed x , a trigger t is reversed by the partial derivative of critical trojan path with respect to x . A testing example x_t is generated by adding the reversed trigger t to the benign seed x . They are calculated as follows:

$$t = \frac{\partial Critical\ Trojan\ Path(x)}{\partial x} \quad (9)$$

$$x_t = \mu \times t + x \quad (10)$$

where ∂ is the partial derivation and $\mu \in [0, 1]$ controls the transparency of the reversed triggers, which is usually set to 0.5. Also, the pixel values of testing examples x_t are limited within the range of $[0, 255]$.

2.6 Trojane Model Detection

The benign seed x and its corresponding testing examples x_t are fed into the model to obtain the model predictions. If there is a change in the model prediction, it indicates a misclassification due to the potential backdoor triggered by the testing example. Hence, we can determine the existence of backdoor in the model according to the label change.

More specifically, we calculate the label change rate (LCR) for the testing examples. Given a set of testing examples $T = \{x_{t1}, x_{t2}, \dots\}$ and a DNN model F . We define LCR on a set of T as follows:

$$LCR = \frac{n_{F(x_t)=c_t}}{N} \quad (11)$$

where N is the total number of testing examples and $n_{F(x_t)=c_t}$ denotes the number of them misclassified as trojan class c_t by the model.

If a model has a potential backdoor, testing examples will trigger high LCR, and vice versa. Considering the influence of false-positive examples, we set the threshold of LCR, $\lambda = 50\%$ for all datasets conducted in our experiment. That is, if more than 50% of the predicted labels turn to one specific label, the model is very likely to be trojaned.

3 EVALUATION

Comprehensive experiments were carried out to verify the performance of CatchBackdoor, including the following aspects:

- **RQ1:** Is LCR a more effective metric for backdoor testing comparing to the traditional testing metrics? Does CatchBackdoor show competitive LCR against various trojan attacks compared with baselines? (Section 3.2)
- **RQ2:** How is the performance of CatchBackdoor in various testing scenarios (i.e., testing without input, adaptive attacks, testing online Model Zoo)? (Section 3.3)
- **RQ3:** Are the generated testing examples helpful in repairing the backdoor model and improving the model robustness against backdoors? (Section 3.4)
- **RQ4:** How is the parameter sensitivity of CatchBackdoor, i.e., k1 and k2? (Section 3.5)
- **RQ5:** Is CatchBackdoor efficient time-cost wise in practice? (Section 3.6)

3.1 Setup

Platform. i7-7700K 4.20GHzx8 (CPU), TITAN Xp 12GiB x2 (GPU), 16GBx4 memory (DDR4), Ubuntu 16.04 (OS), Python 3.6, Tensorflow-gpu-1.10.0.

Datasets. We conduct experiment on MNIST [28], CIFAR-10 [32] and Tiny-ImageNet. MNIST contains 70,000 28×28 gray-scale images, of which 50,000 are used for training, 10,000 for testing. Each image is marked with numbers from 0 to 9. CIFAR-10 includes 60,000 32×32 three-channel RGB-color images, which are divided into ten classes equally. We chose Tiny-ImageNet, a subset of 10 classes of animals in ImageNet [30], containing 13,000 images for evaluation.

Models. For MNIST, we used LeNet family (LeNet-1, LeNet-4, LeNet-5) [29] for trojan testing analysis. On CIFAR-10, AlexNet [33] and ResNet-20 [34] with high training accuracy are adopted. On even larger and more complex datasets Tiny-ImageNet, we adopted VGG16 [35] and VGG19 [35] model. The dataset and its model configurations are shown in Table 1.

Backdoor attacks. We use the neural path to test various types of trojan attacks discussed above, including modification attack, blending attack, neuron hijacking and defense adaptive attack. Modification attacks include dynamic patch (DP) [24], one patch (OP), multiple patches (MP) and irregular patch (IP) [5]. Blending attacks contain Poison Frogs [6] and Hidden trigger [7]. TrojanNN [31], including face stamp and apple stamp, and one defense adaptive attack adversarial embedding attack (ABE) [23], are also conducted in our experiment. We generated 50 benign models and 50 trojaned models. For modification attacks, the poison rates can be 10%, 30%, 50%, or 70%.

Testing baselines. The SOTA detection algorithms ABS [17] and NC [18] are used in our experiments as the baselines. The parameters for these algorithms follow their original experiment settings, respectively.

Metrics and notations: The metrics used in the experiments are defined as follows:

① Classification accuracy: $acc = \frac{N_{true}}{N_{total}}$, where N_{true} is the number of clean examples correctly classified by the targeted model and N_{total} denotes the total number of benign images.

② Attack success rate: $ASR = \frac{N_{adv}}{N}$, where N_{adv} denotes the number of examples misclassified by the targeted model after attacks.

③ Label change rate: $LCR = \frac{n_{F(x_t)=c_t}}{N}$, where N is the total number of testing examples and $F(x_t) = c_t$ denotes the number of them misclassified as trojan class c_t by the model. Methods that could reach higher LCR are more effective in trojaned model detection.

④ Detection rate: $DR = \frac{N_{Tro}}{N_{models}}$, where N_{Tro} denotes the number of trojaned models that could be detected and N_{models} denotes the number of models whose ground truth are trojaned. Noted that DR of various methods could reach nearly 100% in most cases, we use LCR instead in some aspects of result evaluation for a fair comparison.

TABLE 1
Dataset and model configurations.

Dataset	#labels	#Train Inputs	Input size	Model	Params	acc
MNIST	10	50,000	28×28×1	LeNet-1	7,206	95.11%
				LeNet-4	69,362	98.50%
				LeNet-5	107,786	98.90%
CIFAR-10	10	50,000	32×32×3	AlexNet	87,650,186	91.24%
				ResNet-20	273,066	93.04%
Tiny-ImageNet	10	1,281,167	224×224×3	VGG16	134,326,366	95.13%
				VGG19	139,638,622	95.40%

3.2 Testing Example Generation and Trojaned Model Detection

In this section, we mainly focus on analysing whether LCR is a more effective metric for backdoor testing compared to the traditional testing metrics. We also conduct experiments to compare CatchBackdoor with SOTA baselines in trojaned model detection task. Furthermore, we investigate the neuron activations and visualize the testing examples generated by CatchBackdoor in both input feature space and high-dimensional feature space for better understanding.

3.2.1 Results of LCR on trojaned model detection

The existing testing criteria are not suitable for evaluating backdoor testing example generation. Existing white-box testing methods are mainly coverage-based. The state-of-the-art testing criteria [16] are mainly coverage-based as well, e.g., the six metrics introduced in DeepGauge [16], including neuron coverage(NCOV), strong neuron activation coverage(SNAC), k -multisection neuron coverage(TMNC), top- k neuron patterns(TKNP), top- k neuron coverage(TKNC) and neuron boundary coverage(NBC). However, we found that these metrics are of less use when evaluating backdoor testing example generation. As shown in Figure 5, the six metrics are used to evaluate the benign and trojan examples on two trojaned models, i.e., LeNet-5 models of MNIST attacked by Poison Frogs of blending attack and Apple stamps of hijacking attacks. We can see that these metrics barely demonstrate any difference between benign and trojan examples. Similar results are also found using AlexNet on CIFAR-10 and VGG16 on Tiny-ImageNet. Therefore, the existing testing metrics are of little use in evaluating the quality of backdoor testing example generation.

We need a new metric to evaluate the generation quality that can help in distinguishing trojan from benign, i.e. LCR, more details of which are in the following subsections.

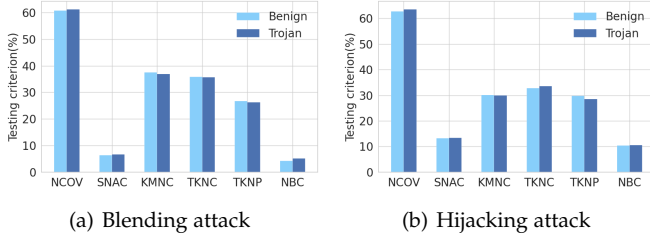


Fig. 5. The six SOTA coverage guided criteria proposed by DeepGauge show little difference between benign and trojan examples, hence are not suitable for evaluating backdoor testing example generation.

CatchBackdoor performance in backdoor detection task. LCR measures the rate that generated testing examples successfully trigger the hidden backdoor in the model. As shown in Figure 6, most trojaned models have much higher LCR than the benign ones. So we believe that LCR is a more suitable evaluation metric for backdoor testing example generation and further an indicator for backdoor detection by finding an appropriate threshold λ of LCR.

We compare CatchBackdoor with the SOTA detection algorithms ABS and NC. The results are shown in Table 2. The two trojan attacks, *i.e.*, blending attack and ABE are used. CatchbBackdoor uses $k_1, k_2 = 3$ in this experiment, and the baselines uses their recommended parameter settings. The LCR in this table is calculated using 100 images per label.

TABLE 2
Comparison of LCR of ABS, NC and CatchBackdoor.

Dataset	Model	Blending attack			ABE		
		ABS	NC	Ours	ABS	NC	Ours
MNIST	LeNet-1	68%	40%	94%	43%	13%	86%
	LeNet-4	79%	37%	91%	41%	20%	87%
	LeNet-5	74%	37%	93%	47%	14%	91%
CIFAR-10	AlexNet	75%	17%	87%	35%	11%	83%
	ResNet-20	77%	17%	88%	38%	7%	85%
Tiny-ImageNet	VGG16	69%	23%	76%	21%	0%	79%
	VGG19	65%	21%	79%	19%	5%	75%

Methods that could reach higher LCR are more effective in trojaned model detection, *i.e.*, the generated examples are more distinct to the benign ones. According to Table 2, CatchBackdoor can effectively trigger more label changes than baselines among all datasets and models. This means that our generated examples can simulate the activation state of the trigger examples in most cases. With λ set at 0.5, almost all trojan potential backdoors for most attack types can be detected, regardless of datasets and model structures.

As for the advanced attack ABE, where the trojan state is not concentrated on a single neuron, CatchBackdoor still performs well by targeting neurons with higher activation frequency. On the contrary, NC and ABS fail to deal with ABE.

However, we have to admit that some trojaned models are still out of our detection since their LCR is lower than 50%, *e.g.*, the three red dots of the Tiny-ImageNet models in Figure 6. The reasons lie in that increasing depth of the model may lead to the redundancy of neurons. Some neuron activation value in the neural path may not be significantly larger than the redundant neurons, which leads to the decrease of LCR for those models.

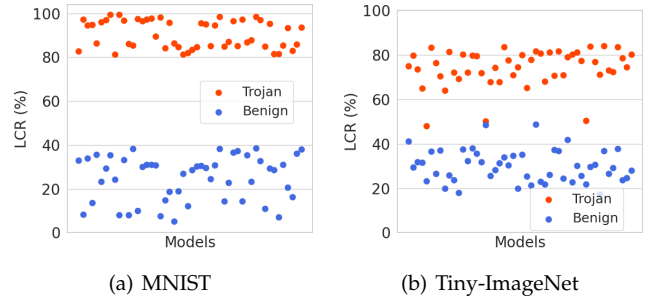


Fig. 6. LCR of benign and trojaned models on different datasets. Red and blue scatters represent LCR results of trojaned and benign models respectively.

3.2.2 Investigation of activations of neurons

To further demonstrate our assumption, we measure the activation value and frequency change for 500 examples. Figure 7 shows the activation value and frequency on different models with different trojan attacks. Green, red and blue bars denote activation value or frequency of 500 benign examples, trojan examples, and testing examples by CatchBackdoor, respectively. We chose the most class-relevant layer (*i.e.*, the penultimate layer) and counted the top-1 neuron activation value and frequency for a fair comparison. The dataset we used for training trojaned models contains 30% trojan examples. The size of DP is 3×3 while MP is 1×1 .

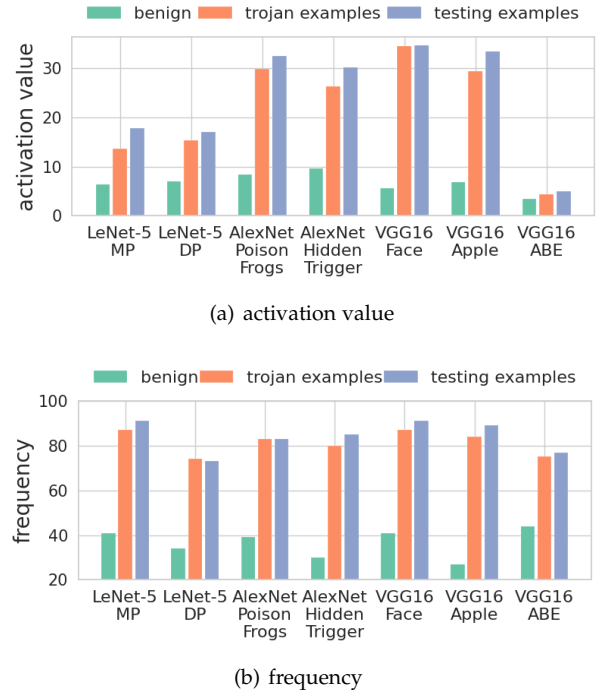


Fig. 7. The activation value and frequency on benign examples, trojan examples, and testing examples by CatchBackdoor.

We can see that the benign and the trojan examples show great difference in both activation value and activation frequency. The activation value and frequency stimulated by our generated examples are close to but higher than those by trojan examples. This well explains the capability of triggering potential backdoors by CatchBackdoor. Consistent with

our assumption, neurons’ activation values increase significantly when backdoors are triggered by trojan examples. Besides, the size and location of patches have little effect on the activation value.

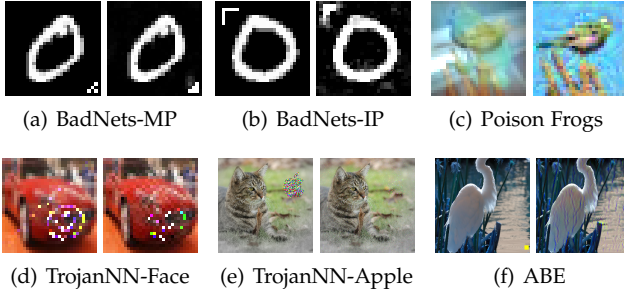


Fig. 8. Visualizations of trojan examples (left) and generated testing examples (right) that change model prediction labels.

3.2.3 Visualization

In order to provide an intuitive understanding of CatchBackdoor, we provide visualization analysis in both input feature space and high-dimensional representative feature space in hidden layers.

Figure 8 shows trojan examples and our generated testing examples under different trojan attacks, i.e., BadNets, Poison Frogs, TrojanNN and ABE. LeNet-5 of MNIST, AlexNet of CIFAR-10 and VGG16 of Tiny-ImageNet are used for visualization. A high visual similarity in appearance and position can be observed from the figures. This well verifies the effectiveness of CatchBackdoor in reversing triggers. Based on the critical trojan path, CatchBackdoor can target more class-related pixels frequently used for classification, which are vulnerable to attacks and may lead to misclassifications.

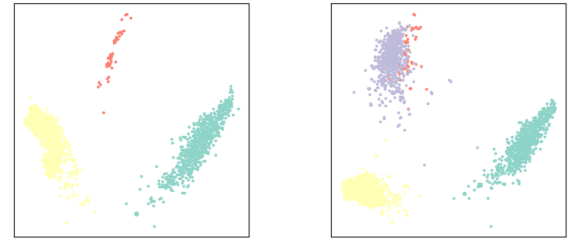
Furthermore, we visualize high-dimensional features via t-SNE [36] on LeNet-5 model under BadNets-MP attack with 10% trojaned examples. The results are shown in Figure 9, where the distribution of trojan examples, testing examples, benign and targeted-class trojan examples are represented by red, purple, yellow, and green clusters, respectively. It can be seen that the well-trained model can distinguish different classes as clusters separate from each other. Testing examples by CatchBackdoor can serve as targeted-class trojan examples to trigger backdoors, as red cluster overlap and purple one. As a result, the testing examples can trigger misclassifications due to backdoors.

Answer to **RQ1**: LCR is a more specific metric for backdoor testing example generation. CatchBackdoor outperforms the SOTA baselines on LCR and hence on backdoor detection by setting an appropriate threshold.

3.3 Testing Example Generation under Various Scenarios

3.3.1 Testing example generation without access to valid input examples

We further investigate the performance of CatchBackdoor when datasets are not available in the testing stage.

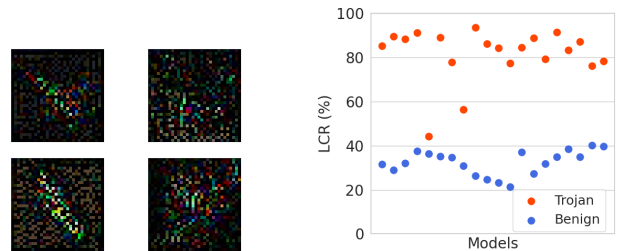


(a) benign and trojan examples (b) benign, trojan, and generated testing examples by CatchBackdoor

Fig. 9. The t-SNE visualization of high-dimensional features of benign, trojan, and generated testing examples by CatchBackdoor.

Instead of using a benign seed, we start with a random noise input examples. We find the critical path by stimulating the model with random noise and determine whether the model is trojaned by generating examples. Testing examples generated on ResNet-20 of CIFAR-10 under Poison Frogs are shown in Figure 10 (a) and the corresponding LCRs are shown in Figure 10 (b).

The same phenomenon could be observed in Figure 10(b) with the scenarios where test datasets are available. LCR of trojaned models and benign ones are rather different. By setting the threshold of LCR at 50%, most trojaned models can still be detected by CatchBackdoor. Two of twenty trojaned models show LCR under 75%. This is because random noise increases the number of neurons triggered by mistakes, confusing the selection of the neural path. CatchBackdoor is able to conduct testing example generation leveraging on the diversity of input examples though they are random noise, which is different from example-free testing.



(a) Generated testing examples

(b) LCR without input

Fig. 10. Generated testing examples by CatchBackdoor and LCR on CIFAR-10 of ResNet-20 without testing inputs.

3.3.2 Testing results of adaptive attacks

A strong assumption on the attacker capability is that the attacker knows the defense mechanism, i.e., how CatchBackdoor works. And hence, the attacker can try to avoid it by adjusting the attack. In this subsection, we evaluate the testing performance under two types of adaptive trojan attacks. We calculate the ASR of these attacks to measure the effectiveness of the adaptive attacks, and the results of LCR to measure the effectiveness of CatchBackdoor, as shown in Table 3.

The first type of adaptive attack, denoted as Type I, minimizes the standard deviation of neuron activation in the same layer during the trojan stage. In Type II attack, triggered neuron activation resembles benign examples' neuron activation as much as possible. With above extra restrictions, a trojan model may need more neurons to achieve trojan behaviors.

TABLE 3
Testing results of adaptive attacks.

Dataset	Model	Type	ASR	LCR	DR
MNIST	LeNet-5	I	91.6%	85.3%	100%
		II	90.4%	85.1%	100%
CIFAR-10	AlexNet	I	88.3%	85.3%	100%
		II	88.5%	85.0%	100%
	ResNet-20	I	87.8%	85.7%	100%
		II	88.4%	86.1%	100%
Tiny-ImageNet	VGG16	I	84.6%	85.1%	100%
		II	86.5%	85.3%	100%
	VGG19	I	85.5%	85.4%	100%
		II	86.1%	85.9%	100%

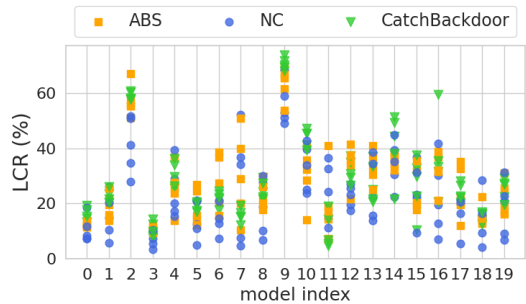
It can be seen from the table the testing performance of our method is still remarkable under adaptive settings, with LCR around 85% and DR up to 100%. Under adaptive settings, multiple neurons achieve trojaned behaviors, and the change of a single one's activation value is not obvious. By selecting those neurons via frequency to generate trojan examples, CatchBackdoor ideally detects backdoors set by adaptive attacks.

3.3.3 Testing online Model Zoo

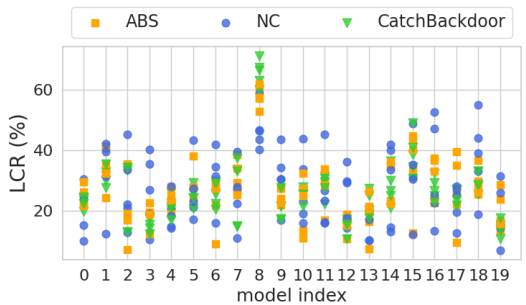
We conducted an experiment on Caffe Model Zoo [4] to apply CatchBackdoor to test pre-trained models. 100 pre-trained models are downloaded for age classification and 100 for gender classification. We experimented 5 rounds to evaluate the potential risks of the models. 1,000 randomly selected examples from each class are reorganized for test sets. We obtained LCR on CatchBackdoor along with the two baselines, ABS and NC. Figure 11 shows the results of 20 models with the highest LCR values of each classification task, where scatters of orange, blue and green denote the LCR of ABS, NC and CatchBackdoor, respectively. Models with larger LCR are more likely to be trojaned (naturally¹ or manually).

According to the figure, compared with baselines, testing examples generated by CatchBackdoor show higher LCR than baselines in most cases. Three methods show the same trend during the testing that No.2 and 9 model in age classification and No.8 in gender are likely to be trojaned, with higher LCR. In the five rounds of testing, all models with potential defects show LCR higher than 50% by CatchBackdoor so that they can be easily detected. This indicates CatchBackdoor can more accurately discover the potential risks of the model. Most models show low LCR among the three methods, so they are prone to be secure for users.

1. A natural backdoor is not implanted manually. Instead, the model may have a specific pattern that can trigger a similar behavior to that of a backdoor trigger.



(a) age



(b) gender

Fig. 11. LCR for Model Zoo Models of age and gender classification

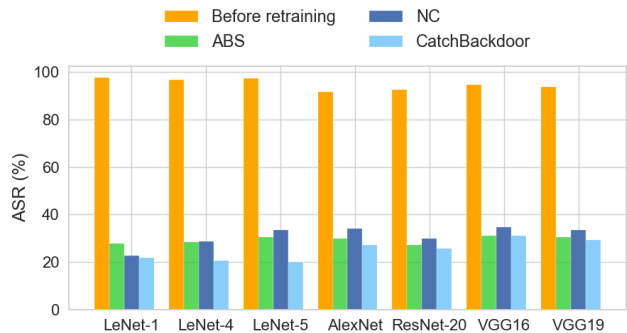


Fig. 12. ASR of modification trojan attacks before and after retraining on different datasets.

Answer to **RQ2**: CatchBackdoor can work well under stricter assumptions when access to valid input examples are unavailable or when attackers design adaptive attacks against CatchBackdoor. We further applied CatchBackdoor to 200 online Model Zoo models, and find 3 models showing suspicious LCRs that need further investigation.

3.4 Robustness Improvement by Retraining DNNs

The testing examples that generated by CatchBackdoor can also be repair the backdoor model by retraining the model using the testing examples. We retrain the model in 20 epochs with 2,000 trojaned examples reversed by the two baselines and CatchBackdoor. The ASR before and after the retraining are shown in Figure 12. Green, navy and lightblue bars denote ASR after retraining with reversed examples by ABS, NC and CatchBackdoor, respectively.

From the figure, we can conclude that retraining can effectively reduce the ASR of trojan attacks. Compared with baselines, models retrained with CatchBackdoor-reversed

examples are more robust against trojan attacks. Trojan examples reversed by CatchBackdoor cover more diverse corner cases that may lead to misclassification. By retaining with those examples, the robustness of models is better enhanced.

Answer to **RQ3**: The robustness of models can be improved up to 60% by retraining DNNs with testing examples generated by CatchBackdoor, better than that generated by baselines.

3.5 Parameter Sensitivity Analysis (k_1 and k_2)

k_1 and k_2 are two important parameters of CatchBackdoor. This subsection analyses the parameter sensitivity. The two parameters controls the path selection of the convolution layers and fully connected layers, respectively. We measure the LCR of testing examples generated under different k_1 and k_2 , as shown in Figure 13.

The increase of k_1 and k_2 can effectively raise the value of LCR and the confidence of whether the model is trojaned. Concretely, the modification of k_2 has a more significant impact on LCR than k_1 . It may go to the fact that the fully connected layers are relatively close to the output layer, and the extracted high-dimensional features are more effective for classification.

For the advanced trojan attacks (*i.e.*, ABE), we find that the testing examples generated by only a single neuron cannot achieve high LCR. Trojaned behaviors are produced by the joint action of multiple neurons. This is in line with the definition of the neural path. DNNs should be a whole and work together to achieve the effect of classification.

It is worth noting that a larger value of k is not related to better an effect. With the increase of k_1 and k_2 , neural path selection will be more time-consuming, for too many redundant neurons are introduced.

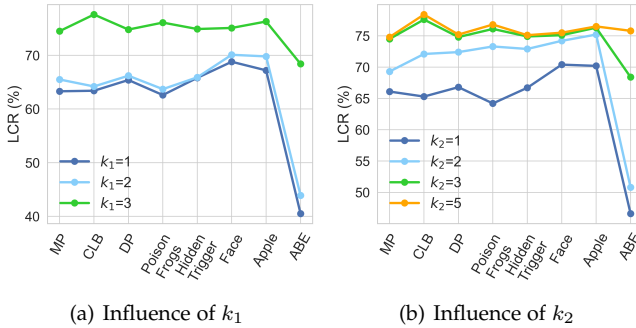


Fig. 13. The results of LCR on Tiny-ImageNet under different k_1 and k_2 , where abscissa denotes different trojan attacks.

Answer to **RQ4**: Parameter k_1 and k_2 work together to guarantee the detection performance of CatchBackdoor. Specifically, k_2 contributes more to LCR than k_1 .

3.6 Time Complexity

To measure the efficiency of CatchBackdoor, we compare the time cost of ABS, NC, and CatchBackdoor. The time costs for generating 100 testing examples are shown in Table 4. In our experiment, all three methods use the same set of input examples that cover a variety of classes. Both of k_1 and k_2 are set to 1.

TABLE 4
Time Cost Comparison of ABS, NC and ours.

Dataset	Model	Time(s)		
		ABS	NC	CatchBackdoor
MNIST	LeNet-1	80	300	100
	LeNet-4	85	510	115
	LeNet-5	85	630	115
CIFAR-10	AlexNet	460	13780	460
	ResNet-20	990	27150	850
Tiny-ImageNet	VGG16	780	Timeout	6620
	VGG19	810	Timeout	7960

According to the Table 4, it is evident that the CatchBackdoor shows low computation time among baselines in most situations. In small datasets, CatchBackdoor is slightly inferior to ABS, but is still much faster than NC. The reason is that CatchBackdoor fuzzes diversity inputs to observe the internals while NC must scan all the output class labels one by one and construct the minimum perturbation for each class label. With the increasing of model complexity, the time cost of CatchBackdoor increases (the complexity of the model combined with datasets order is VGG>ResNet>AlexNet>LeNet in this setting) due to the increase of the total number of neurons.

Answer to **RQ5**: Compared with baselines, our method achieves relatively low time complexity and high efficiency in most cases.

4 THREATS TO VALIDITY

CatchBackdoor triggers trojaned behaviors for backdoor detection by controlling the top- k neural path. However, these paths may not cover all corner cases. There is potential possibility that CatchBackdoor may have false negatives.

For feature space trojan attacks, it is difficult to reverse a visually sensible trigger for the reason that the trojan examples are visually similar to the benign examples. However, CatchBackdoor has demonstrated its capability in detecting such trojan attack, *i.e.*, Poison Frogs and Hidden Triggers.

Besides, the threats to internal validity also come from the erroneous experiments and the replication of the baseline methods. We compare DR, LCR and time complexity with the state-of-the-art detection methods, NC and ABS. We strictly follow the procedures described in their work and re-implemented our versions of the baselines. However, our method may not completely restore the selection of examples in NC and simulation steps of ABS.

Threats to external validity lie in whether our approach can be transferable to other scenarios. In our experiment, unavailable testing data and online pre-trained models are included. Detection on other DL systems, such as RNN and GNN would be validated in the future.

5 RELATED WORK

This section, we will briefly introduce the trojan attacks, detection, and testing methods of DNNs. Besides, neuron-level approaches for DNNs in security domains are introduced as well.

5.1 Trojan Attacks

Trojan attack injects hidden malicious backdoors into the model, which can cause misclassification when the input contains a specific pattern called a trigger. In general, they could be categorized into four types: modification attacks, blending attacks, neuron hijacking, and defense adaptive trojan attacks.

Modification attack. Modification attacks mainly modify a single pixel or a pattern on images to reach trojan effects. BadNets [5] adds triggers to examples and injects label pairs into the training set to train victim models. Dynamic backdoor [24] crafts pattern and position dynamically to reduce the efficacy. Clean-label backdoor (CLB) [25] generates stealthy trojan inputs through adversarial perturbations or generative networks.

Blending attack. Blending attacks mainly blend one class latent representation to other classes. Poison frogs [6] blends target class images as a watermark into benign class images. Hidden trigger backdoor [7] joints pixel and feature space to generate trojan examples close to target examples. Besides, Refool [27] adopts the physical concept reflection to optimizes trigger stealthiness.

Neuron hijacking. Neuron hijacking attacks mainly optimize pre-defined triggers combined with specific neurons. TrojanNN [31] access the training parameters and place potential backdoors into pre-trained models. DeepPayload [37] achieves backdoor attack after resizing operation by a malicious payload.

Defense adaptive attacks. Defense adaptive attacks optimize triggers to evade possible defenses. ABE [23] minimizes the difference in latent representations of trojan and benign inputs. IMC [10] achieves adaptive attacks by optimizing trojan stamps and weights jointly.

5.2 Detection Methods For Trojan Attacks

Several detection approaches have been studied to hunt trojan attacks. They determine whether the model is trojaned by different means.

STRIP [19] accesses training data to check whether the inputs are trojaned during run-time. It has a good effect when detecting single target class trojan attacks but fail to handle all-to-all attack labels, where both the trigger pattern and the original input class need to be recognized. Activation clustering (AC) [21] uses K-means clustering to separate benign and trojan data. It can not be applied to neuron hijacking. Spectral signature (SS) [20] uses singular value decomposition and removes those that possibly contain trojan triggers. SS focuses on the distribution of examples, so it fails to detect neuron hijacking. Neural cleanse (NC) [18] uses a reverse engineering process to find the minimum perturbations, likely to be the injected backdoor triggers for each label. It fails to work in scenarios with less than three classes and all-to-all attacks. Artificial brain stimulation (ABS) [17] performs detection by finding compromised neuron candidates through a stimulation method. It further reverses the trigger pattern to decide whether the model is trojaned. It shows limitations on scenarios without evidence of compromised neurons, e.g., feature space attacks [6], [7]. EX-RAY [22] can distinguish natural features from trojan features, based on the symmetric feature differencing

method. But it shows weakness in reversing triggers of blending attacks and defense adaptive attacks.

5.3 Testing Approaches For DNNs

Testing methods achieve the goal via generating testing examples against various trojan attacks. They could be divided into black-box and white-box methods. The former achieve testing without observing the internal behaviors of models while the latter from the perspective of model inside. The state-of-the-art testing approaches of DNNs draw lessons from the traditional software testing [38], [39], [40], [41] methods, suitable for large dimension and potential testing space.

Black-box testing methods. Wicker et al. [42] proposed a “Scale Invariant Feature Transform” feature guided black-box testing and showed its competitiveness with C&W [43] and JSMA [44] attacks. DeepMutation [45] mutates DNNs (i.e., injecting faults either from the source level or model level) to evaluate the test data quality. Robustness-oriented testing framework RobOT [46] proposes first-order loss, and uses it to generate testing examples to improve model robustness.

White-box testing methods. Here we mainly focus on methods based on coverage criterion. DeepXplore [47] introduces neuron coverage to measure the amount of tested logic inside the model to systematically find inputs that can trigger multiple models’ inconsistencies. DeepGauge [16] proposes a set of multi-granularity testing criteria, providing various testing descriptions at a more fine-grained level. DeepHunter [48] uses multi-granularity criterion feedback to guide the generation of testing examples, to realize deep exploration of models. DeepCT [49] adapts the concept of combinatorial testing and provides a set of coverage based on each layer’s neuron input interaction. Inspired by the MC/DC test criteria in traditional software [50]. Sun et al. [51] proposed a set of adapted MC/DC test criteria for DNNs. Lee et al. [52] propose ADAPT that can adaptively determine neuron-selection strategies during testing.

5.4 Neuron-level Approaches for DNNs in Security Domains

Several methods related to neuron behaviors have been put forward for the security of DNNs.

Adversarial defense. Zhang et al. [53] explained the adversarial robustness from neuron sensitivity, measured by changes of neuron behaviors against benign and adversarial examples. In the adversarial setting, Li et al. [54] computed the gradients between neurons during backward-propagation and linked neurons with higher gradients to compose the critical attacking route in the adversarial setting. Model robustness can be improved by constraining the propagation process and neuron behaviors on this route.

Adversarial detection. Ma et al. [55] observed changes on neuron activation values under various adversarial attacks. They proposed the value invariants and the provenance invariants for adversarial detection. Besides, Shan et al. [56] injected trapdoors and honeypot into the data. By comparing the signal of input neuron activation and the trapdoor, adversarial attacks could be detected.

From the view of neurons inside, the works mentioned above achieve successful adversarial detection or defense for DNNs. But they show limitations in trojan settings.

6 LIMITATIONS AND CONCLUSIONS

This paper proposes the concept of critical trojan neural path and develops a white-box trojan testing method CatchBackdoor. Via differential fuzzing of critical neurons from a small number of benign examples, we identify the trojan paths and particularly the critical ones, and generate backdoor testing examples by simulating the critical neurons in the identified paths. Leveraging on these testing examples, we can successfully detect a variety of trojan attacks.

However, it still has some limitations. As for computation cost, the complexity can be further reduced when applied to complex models with more layers. A more lightweight path selection strategy is required to alleviate the impact of redundant neurons and improve the efficiency of critical neuron selection. Besides, we will work towards handling trojan attacks without triggers, i.e., mislabel attacks. CatchBackdoor will cover more kinds of trojan attacks in the future. We hope that our approach can be applied in scenarios in the real world, such as autonomous driving, face recognition, and other security domains.

REFERENCES

- [1] O. M. Parkhi, A. Vedaldi, and A. Zisserman, "Deep face recognition," 2015.
- [2] J. Redmon, S. K. Divvala, R. B. Girshick, and A. Farhadi, "You only look once: Unified, real-time object detection," *CoRR*, vol. abs/1506.02640, 2015. [Online]. Available: <http://arxiv.org/abs/1506.02640>
- [3] H. Gudaparthi, R. Johnson, H. Challa, and N. Niu, "Deep learning for smart sewer systems: assessing nonfunctional requirements," in *ICSE-SEIS '20: Proceedings of the ACM/IEEE 42nd International Conference on Software Engineering: Software Engineering in Society, Seoul, South Korea, 27 June - 19 July, 2020*, G. Rothermel and D. Bae, Eds. ACM, 2020, pp. 35–38. [Online]. Available: <https://doi.org/10.1145/3377815.3381379>
- [4] Y. D. Chun, S. Y. Seo, and N. C. Kim, "Image retrieval using BDIP and BVLC moments," *IEEE Trans. Circuits Syst. Video Technol.*, vol. 13, no. 9, pp. 951–957, 2003. [Online]. Available: <https://doi.org/10.1109/TCSVT.2003.816507>
- [5] T. Gu, B. Dolan-Gavitt, and S. Garg, "Badnets: Identifying vulnerabilities in the machine learning model supply chain," *CoRR*, vol. abs/1708.06733, 2017. [Online]. Available: <http://arxiv.org/abs/1708.06733>
- [6] A. Shafahi, W. R. Huang, M. Najibi, O. Suci, C. Studer, T. Dumitras, and T. Goldstein, "Poison frogs! targeted clean-label poisoning attacks on neural networks," in *Advances in Neural Information Processing Systems*, 2018, pp. 6103–6113.
- [7] A. Saha, A. Subramanya, and H. Pirsiavash, "Hidden trigger backdoor attacks," in *Proceedings of the AAAI Conference on Artificial Intelligence*, vol. 34, no. 07, 2020, pp. 11 957–11 965.
- [8] E. Bagdasaryan, A. Veit, Y. Hua, D. Estrin, and V. Shmatikov, "How to backdoor federated learning," in *The 23rd International Conference on Artificial Intelligence and Statistics, AISTATS 2020, 26-28 August 2020, Online [Palermo, Sicily, Italy]*, ser. Proceedings of Machine Learning Research, S. Chiappa and R. Calandra, Eds., vol. 108. PMLR, 2020, pp. 2938–2948. [Online]. Available: <http://proceedings.mlr.press/v108/bagdasaryan20a.html>
- [9] S. Gerasimou, H. F. Eniser, A. Sen, and A. Cakan, "Importance-driven deep learning system testing," in *ICSE '20: 42nd International Conference on Software Engineering, Seoul, South Korea, 27 June - 19 July, 2020*, G. Rothermel and D. Bae, Eds. ACM, 2020, pp. 702–713. [Online]. Available: <https://doi.org/10.1145/3377811.3380391>
- [10] R. Pang, H. Shen, X. Zhang, S. Ji, Y. Vorobeychik, X. Luo, A. X. Liu, and T. Wang, "A tale of evil twins: Adversarial inputs versus poisoned models," in *CCS '20: 2020 ACM SIGSAC Conference on Computer and Communications Security, Virtual Event, USA, November 9-13, 2020*, J. Ligatti, X. Ou, J. Katz, and G. Vigna, Eds. ACM, 2020, pp. 85–99. [Online]. Available: <https://doi.org/10.1145/3372297.3417253>
- [11] R. Gopinath, C. Jensen, and A. Groce, "Code coverage for suite evaluation by developers," in *36th International Conference on Software Engineering, ICSE '14, Hyderabad, India - May 31 - June 07, 2014*, P. Jalote, L. C. Briand, and A. van der Hoek, Eds. ACM, 2014, pp. 72–82. [Online]. Available: <https://doi.org/10.1145/2568225.2568278>
- [12] S. Berner, R. Weber, and R. K. Keller, "Enhancing software testing by judicious use of code coverage information," in *29th International Conference on Software Engineering (ICSE 2007), Minneapolis, MN, USA, May 20-26, 2007*. IEEE Computer Society, 2007, pp. 612–620. [Online]. Available: <https://doi.org/10.1109/ICSE.2007.34>
- [13] S. Scalabrino, G. Bavota, C. Vendome, M. L. Vásquez, D. Poshyvanyk, and R. Oliveto, "Automatically assessing code understandability: how far are we?" in *Proceedings of the 32nd IEEE/ACM International Conference on Automated Software Engineering, ASE 2017, Urbana, IL, USA, October 30 - November 03, 2017*, G. Rosu, M. D. Penta, and T. N. Nguyen, Eds. IEEE Computer Society, 2017, pp. 417–427. [Online]. Available: <https://doi.org/10.1109/ASE.2017.8115654>
- [14] J. Chen, G. Wang, D. Hao, Y. Xiong, H. Zhang, L. Zhang, and B. Xie, "Coverage prediction for accelerating compiler testing," *IEEE Trans. Software Eng.*, vol. 47, no. 2, pp. 261–278, 2021. [Online]. Available: <https://doi.org/10.1109/TSE.2018.2889771>
- [15] C. J. Budnik, M. Gario, G. Markov, and Z. Wang, "Guided test case generation through AI enabled output space exploration," in *Proceedings of the 13th International Workshop on Automation of Software Test, AST@ICSE 2018, Gothenburg, Sweden, May 28-29, 2018*, X. Bai, J. J. Li, and A. Ulrich, Eds. ACM, 2018, pp. 53–56. [Online]. Available: <https://doi.org/10.1145/3194733.3194740>
- [16] L. Ma, F. Juefei-Xu, F. Zhang, J. Sun, M. Xue, B. Li, C. Chen, T. Su, L. Li, Y. Liu, J. Zhao, and Y. Wang, "Deepgaue: multi-granularity testing criteria for deep learning systems," in *Proceedings of the 33rd ACM/IEEE International Conference on Automated Software Engineering, ASE 2018, Montpellier, France, September 3-7, 2018*, M. Huchard, C. Kästner, and G. Fraser, Eds. ACM, 2018, pp. 120–131. [Online]. Available: <https://doi.org/10.1145/3238147.3238202>
- [17] Y. Liu, W. Lee, G. Tao, S. Ma, Y. Aafer, and X. Zhang, "ABS: scanning neural networks for back-doors by artificial brain stimulation," in *Proceedings of the 2019 ACM SIGSAC Conference on Computer and Communications Security, CCS 2019, London, UK, November 11-15, 2019*, L. Cavallaro, J. Kinder, X. Wang, and J. Katz, Eds. ACM, 2019, pp. 1265–1282. [Online]. Available: <https://doi.org/10.1145/3319535.3363216>
- [18] B. Wang, Y. Yao, S. Shan, H. Li, B. Viswanath, H. Zheng, and B. Y. Zhao, "Neural cleanse: Identifying and mitigating backdoor attacks in neural networks," in *2019 IEEE Symposium on Security and Privacy, SP 2019, San Francisco, CA, USA, May 19-23, 2019*. IEEE, 2019, pp. 707–723. [Online]. Available: <https://doi.org/10.1109/SP.2019.00031>
- [19] Y. Gao, C. Xu, D. Wang, S. Chen, D. C. Ranasinghe, and S. Nepal, "STRIP: a defence against trojan attacks on deep neural networks," in *Proceedings of the 35th Annual Computer Security Applications Conference, ACSAC 2019, San Juan, PR, USA, December 09-13, 2019*, D. Balenson, Ed. ACM, 2019, pp. 113–125. [Online]. Available: <https://doi.org/10.1145/3359789.3359790>
- [20] R. M. Hoffer and C. J. Johansson, "Ecological potentials in spectral signature analysis," pp. 1–16, 1969.
- [21] B. Chen, W. Carvalho, N. Baracaldo, H. Ludwig, B. Edwards, T. Lee, I. M. Molloy, and B. Srivastava, "Detecting backdoor attacks on deep neural networks by activation clustering," in *Workshop on Artificial Intelligence Safety 2019 co-located with the Thirty-Third AAAI Conference on Artificial Intelligence 2019 (AAAI-19), Honolulu, Hawaii, January 27, 2019*, ser. CEUR Workshop Proceedings, H. Espinoza, S. Ó. hÉigeartaigh, X. Huang, J. Hernández-Orallo, and M. Castillo-Effen, Eds., vol. 2301. CEUR-WS.org, 2019. [Online]. Available: http://ceur-ws.org/Vol-2301/paper_18.pdf
- [22] Y. Liu, G. Shen, G. Tao, Z. Wang, S. Ma, and X. Zhang, "EX-RAY: distinguishing injected backdoor from natural features

- in neural networks by examining differential feature symmetry," *CoRR*, vol. abs/2103.08820, 2021. [Online]. Available: <https://arxiv.org/abs/2103.08820>
- [23] T. J. L. Tan and R. Shokri, "Bypassing backdoor detection algorithms in deep learning," in *IEEE European Symposium on Security and Privacy, EuroS&P 2020, Genoa, Italy, September 7-11, 2020*. IEEE, 2020, pp. 175–183. [Online]. Available: <https://doi.org/10.1109/EuroSP48549.2020.00019>
- [24] A. Salem, R. Wen, M. Backes, S. Ma, and Y. Zhang, "Dynamic backdoor attacks against machine learning models," *CoRR*, vol. abs/2003.03675, 2020. [Online]. Available: <https://arxiv.org/abs/2003.03675>
- [25] S. Zhao, X. Ma, X. Zheng, J. Bailey, J. Chen, and Y. Jiang, "Clean-label backdoor attacks on video recognition models," in *2020 IEEE/CVF Conference on Computer Vision and Pattern Recognition, CVPR 2020, Seattle, WA, USA, June 13-19, 2020*. Computer Vision Foundation / IEEE, 2020, pp. 14 431–14 440. [Online]. Available: https://openaccess.thecvf.com/content_CVPR_2020/html/Zhao_Clean-Label_Backdoor_Attacks_on_Video_Recognition_Models_CVPR_2020_paper.html
- [26] X. Chen, C. Liu, B. Li, K. Lu, and D. Song, "Targeted backdoor attacks on deep learning systems using data poisoning," *CoRR*, vol. abs/1712.05526, 2017. [Online]. Available: <http://arxiv.org/abs/1712.05526>
- [27] Y. Liu, X. Ma, J. Bailey, and F. Lu, "Reflection backdoor: A natural backdoor attack on deep neural networks," in *Computer Vision - ECCV 2020 - 16th European Conference, Glasgow, UK, August 23-28, 2020, Proceedings, Part X*, ser. Lecture Notes in Computer Science, A. Vedaldi, H. Bischof, T. Brox, and J. Frahm, Eds., vol. 12355. Springer, 2020, pp. 182–199. [Online]. Available: https://doi.org/10.1007/978-3-030-58607-2_11
- [28] Y. LeCun, L. Bottou, Y. Bengio, and P. Haffner, "Gradient-based learning applied to document recognition," *Proceedings of the IEEE*, vol. 86, no. 11, pp. 2278–2324, 1998.
- [29] Y. LeCun *et al.*, "Lenet-5, convolutional neural networks," URL: <http://yann.lecun.com/exdb/lenet>, vol. 20, no. 5, p. 14, 2015.
- [30] O. Russakovsky, J. Deng, H. Su, J. Krause, S. Satheesh, S. Ma, Z. Huang, A. Karpathy, A. Khosla, M. S. Bernstein, A. C. Berg, and F. Li, "Imagenet large scale visual recognition challenge," *Int. J. Comput. Vis.*, vol. 115, no. 3, pp. 211–252, 2015. [Online]. Available: <https://doi.org/10.1007/s11263-015-0816-y>
- [31] Y. Liu, S. Ma, Y. Aafer, W. Lee, J. Zhai, W. Wang, and X. Zhang, "Trojaning attack on neural networks," in *25th Annual Network and Distributed System Security Symposium, NDSS 2018, San Diego, California, USA, February 18-21, 2018*. The Internet Society, 2018. [Online]. Available: http://wp.internetsociety.org/ndss/wp-content/uploads/sites/25/2018/02/ndss2018_03A-5_Liu_paper.pdf
- [32] A. Krizhevsky, G. Hinton *et al.*, "Learning multiple layers of features from tiny images," 2009.
- [33] A. Krizhevsky, I. Sutskever, and G. E. Hinton, "Imagenet classification with deep convolutional neural networks," *Communications of the ACM*, vol. 60, no. 6, pp. 84–90, 2017.
- [34] K. He, X. Zhang, S. Ren, and J. Sun, "Deep residual learning for image recognition," in *2016 IEEE Conference on Computer Vision and Pattern Recognition, CVPR 2016, Las Vegas, NV, USA, June 27-30, 2016*. IEEE Computer Society, 2016, pp. 770–778. [Online]. Available: <https://doi.org/10.1109/CVPR.2016.90>
- [35] K. Simonyan and A. Zisserman, "Very deep convolutional networks for large-scale image recognition," in *3rd International Conference on Learning Representations, ICLR 2015, San Diego, CA, USA, May 7-9, 2015, Conference Track Proceedings*, Y. Bengio and Y. LeCun, Eds., 2015. [Online]. Available: <http://arxiv.org/abs/1409.1556>
- [36] L. Van der Maaten and G. Hinton, "Visualizing data using t-sne," *Journal of machine learning research*, vol. 9, no. 11, 2008.
- [37] Y. Li, J. Hua, H. Wang, C. Chen, and Y. Liu, "Deeppayload: Black-box backdoor attack on deep learning models through neural payload injection," in *43rd IEEE/ACM International Conference on Software Engineering, ICSE 2021, Madrid, Spain, 22-30 May 2021*. IEEE, 2021, pp. 263–274. [Online]. Available: <https://doi.org/10.1109/ICSE43902.2021.00035>
- [38] B. Baudry and M. Monperrus, "The multiple facets of software diversity: Recent developments in year 2000 and beyond," *ACM Comput. Surv.*, vol. 48, no. 1, pp. 16:1–16:26, 2015. [Online]. Available: <https://doi.org/10.1145/2807593>
- [39] R. Feldt, R. Torkar, T. Gorschek, and W. Afzal, "Searching for cognitively diverse tests: Towards universal test diversity metrics," in *First International Conference on Software Testing Verification and Validation, ICST 2008, Lillehammer, Norway, April 9-11, 2008, Workshops Proceedings*. IEEE Computer Society, 2008, pp. 178–186. [Online]. Available: <https://doi.org/10.1109/ICSTW.2008.36>
- [40] G. Fraser and A. Arcuri, "Whole test suite generation," *IEEE Trans. Software Eng.*, vol. 39, no. 2, pp. 276–291, 2013. [Online]. Available: <https://doi.org/10.1109/TSE.2012.14>
- [41] L. Ma, C. Artho, C. Zhang, H. Sato, J. Gmeiner, and R. Ramler, "GRT: program-analysis-guided random testing (T)," in *30th IEEE/ACM International Conference on Automated Software Engineering, ASE 2015, Lincoln, NE, USA, November 9-13, 2015*, M. B. Cohen, L. Grunske, and M. Whalen, Eds. IEEE Computer Society, 2015, pp. 212–223. [Online]. Available: <https://doi.org/10.1109/ASE.2015.49>
- [42] M. Wicker, X. Huang, and M. Kwiatkowska, "Feature-guided black-box safety testing of deep neural networks," in *Tools and Algorithms for the Construction and Analysis of Systems - 24th International Conference, TACAS 2018, Held as Part of the European Joint Conferences on Theory and Practice of Software, ETAPS 2018, Thessaloniki, Greece, April 14-20, 2018, Proceedings, Part I*, ser. Lecture Notes in Computer Science, D. Beyer and M. Huisman, Eds., vol. 10805. Springer, 2018, pp. 408–426. [Online]. Available: https://doi.org/10.1007/978-3-319-89960-2_22
- [43] N. Carlini and D. A. Wagner, "Towards evaluating the robustness of neural networks," in *2017 IEEE Symposium on Security and Privacy, SP 2017, San Jose, CA, USA, May 22-26, 2017*. IEEE Computer Society, 2017, pp. 39–57. [Online]. Available: <https://doi.org/10.1109/SP.2017.49>
- [44] N. Papernot, P. D. McDaniel, S. Jha, M. Fredrikson, Z. B. Celik, and A. Swami, "The limitations of deep learning in adversarial settings," in *IEEE European Symposium on Security and Privacy, EuroS&P 2016, Saarbrücken, Germany, March 21-24, 2016*. IEEE, 2016, pp. 372–387. [Online]. Available: <https://doi.org/10.1109/EuroSP.2016.36>
- [45] L. Ma, F. Zhang, J. Sun, M. Xue, B. Li, F. Juefei-Xu, C. Xie, L. Li, Y. Liu, J. Zhao, and Y. Wang, "Deepmutation: Mutation testing of deep learning systems," *CoRR*, vol. abs/1805.05206, 2018. [Online]. Available: <http://arxiv.org/abs/1805.05206>
- [46] J. Wang, J. Chen, Y. Sun, X. Ma, D. Wang, J. Sun, and P. Cheng, "Robot: Robustness-oriented testing for deep learning systems," in *43rd IEEE/ACM International Conference on Software Engineering, ICSE 2021, Madrid, Spain, 22-30 May 2021*. IEEE, 2021, pp. 300–311. [Online]. Available: <https://doi.org/10.1109/ICSE43902.2021.00038>
- [47] K. Pei, Y. Cao, J. Yang, and S. Jana, "Deepxplore: automated whitebox testing of deep learning systems," *Commun. ACM*, vol. 62, no. 11, pp. 137–145, 2019. [Online]. Available: <https://doi.org/10.1145/3361566>
- [48] X. Xie, L. Ma, F. Juefei-Xu, M. Xue, H. Chen, Y. Liu, J. Zhao, B. Li, J. Yin, and S. See, "Deephunter: a coverage-guided fuzz testing framework for deep neural networks," in *Proceedings of the 28th ACM SIGSOFT International Symposium on Software Testing and Analysis, ISSA 2019, Beijing, China, July 15-19, 2019*, D. Zhang and A. Möller, Eds. ACM, 2019, pp. 146–157. [Online]. Available: <https://doi.org/10.1145/3293882.3330579>
- [49] L. Ma, F. Juefei-Xu, M. Xue, B. Li, L. Li, Y. Liu, and J. Zhao, "Deepct: Tomographic combinatorial testing for deep learning systems," in *26th IEEE International Conference on Software Analysis, Evolution and Reengineering, SANER 2019, Hangzhou, China, February 24-27, 2019*, X. Wang, D. Lo, and E. Shihab, Eds. IEEE, 2019, pp. 614–618. [Online]. Available: <https://doi.org/10.1109/SANER.2019.8668044>
- [50] K. J. Hayhurst, *A practical tutorial on modified condition/decision coverage*. DIANE Publishing, 2001.
- [51] Y. Sun, X. Huang, and D. Kroening, "Testing deep neural networks," *CoRR*, vol. abs/1803.04792, 2018. [Online]. Available: <http://arxiv.org/abs/1803.04792>
- [52] S. Lee, S. Cha, D. Lee, and H. Oh, "Effective white-box testing of deep neural networks with adaptive neuron-selection strategy," in *ISSA '20: 29th ACM SIGSOFT International Symposium on Software Testing and Analysis, Virtual Event, USA, July 18-22, 2020*, S. Khurshid and C. S. Pasareanu, Eds. ACM, 2020, pp. 165–176. [Online]. Available: <https://doi.org/10.1145/3395363.3397346>
- [53] C. Zhang, A. Liu, X. Liu, Y. Xu, H. Yu, Y. Ma, and T. Li,

- “Interpreting and improving adversarial robustness of deep neural networks with neuron sensitivity,” *IEEE Trans. Image Process.*, vol. 30, pp. 1291–1304, 2021. [Online]. Available: <https://doi.org/10.1109/TIP.2020.3042083>
- [54] T. Li, A. Liu, X. Liu, Y. Xu, C. Zhang, and X. Xie, “Understanding adversarial robustness via critical attacking route,” *Inf. Sci.*, vol. 547, pp. 568–578, 2021. [Online]. Available: <https://doi.org/10.1016/j.ins.2020.08.043>
- [55] S. Ma, Y. Liu, G. Tao, W. Lee, and X. Zhang, “NIC: detecting adversarial samples with neural network invariant checking,” in *26th Annual Network and Distributed System Security Symposium, NDSS 2019, San Diego, California, USA, February 24-27, 2019*. The Internet Society, 2019. [Online]. Available: <https://www.ndss-symposium.org/ndss-paper/nic-detecting-adversarial-samples-with-neural-network-invariant-checking/>
- [56] S. Shan, E. Wenger, B. Wang, B. Li, H. Zheng, and B. Y. Zhao, “Gotta catch ‘em all: Using honeypots to catch adversarial attacks on neural networks,” in *CCS ’20: 2020 ACM SIGSAC Conference on Computer and Communications Security, Virtual Event, USA, November 9-13, 2020*, J. Ligatti, X. Ou, J. Katz, and G. Vigna, Eds. ACM, 2020, pp. 67–83. [Online]. Available: <https://doi.org/10.1145/3372297.3417231>